Highly Active Fenton-Like Catalyst Derived from Solid Waste-Iron Ore Tailings Using Wheat Straw Pyrolysis

Lihui Gao
China University of Mining and Technology
Lizhang Wang
China University of Mining and Technology
Shulei Li
China University of Mining and Technology
Yijun Cao (caoyijuncumt@163.com)
Zhengzhou University

Research Article

Keywords: Iron ore tailings, Wheat straw, Heterogeneous catalyst, Biochar, Decomposition rate

Posted Date: June 24th, 2021

DOI: https://doi.org/10.21203/rs.3.rs-472422/v1

Highly active Fenton-like catalyst derived from solid waste-iron ore tailings using wheat straw pyrolysis

Lihui Gao[1]; Lizhang Wang[1]; Shulei Li[2*]; Yijun Cao[2,3*]

1. School of Environment and Spatial Informatics, China University of Mining and Technology, Xuzhou 221116, China
2. National Engineering Research Center of Coal Preparation and Purification, China University of Mining and Technology, Xuzhou 221116, China
3. School of Chemical Engineering and Technology, Zhengzhou University, Zhengzhou 450001, China

Abstract: The pollutants degradation rate of iron ore tailings-based heterogeneous catalysts is the main factor limiting its application. Herein, an iron ore tailings-based Fenton-like catalyst(I/W(3:1)-900-60) with relative fast catalysis rate was constructed by co-pyrolysis(900 ℃, 60min holding time) of iron ore tailings and wheat straw with mass ratio of 3:1. With wheat straw blending, the generated I/W(3:1)-900-60 presented a larger surface area(24.3 m^2/g), smaller pore size(3.707 nm), reduced iron species (Fe^{2+} from magnetic) and a higher catalytic activity(0.0229 min^{-1}) than I-900-60 (1.196 m^2/g, 12.935 nm, 0.012 min^{-1}) pyrolyzed using a single iron ore tailings under the same pyrolysis conditions. In addition, biochar and iron ore tailings in I/W(3:1)-900-60 were tightly combined through chemical bonding. The optimal catalyst remains active after three cycles, indicating its catalytic stability and recyclability. The good Fenton-like MB degradation efficiency of I/W(3:1)-900-60 was ascribed to the sacrificial role of biochar, as well as the electron transfer between biochar and iron active sites or the

To whom correspondence should be addressed (caoyijun@163.com; lishuleibgs@163.com)

redox cycles of $\equiv Fe^{3+}/Fe^{2+}$. This finding provides a facile construction strategy for a highly active iron ore tailings-based Fenton-like catalyst, and thereby had a great potential application in wastewater treatment.

Key words: Iron ore tailings; Wheat straw; Heterogeneous catalyst; Biochar; Decomposition rate

1. Introduction

Mining industry is an important activity to extract mineral products around the world. Nevertheless, the mining process always brings a certain degree of pollution. Tailings are solid waste remaining after mining valuable minerals, which are usually disposed at waste dams or landfills that present potential environmental damage (Rico et al. 2008; Kossoff et al. 2014). In March 2020, a miserable accident involving a waste dam occurred when the Yichun waste dam (Harbin, China) for the storage of iron ore tailings collapsed. This accident caused 60,000 m^3 of mining tailings disclosing and 3 million m^3 of wastewater releasing, leading to 70 kilometers of river pollution and serious economic loss. A number of other tailings dam accidents have occurred in different countries (Batista et al. 2020) . According to statistics (Yi et al. 2020), the accumulated of tailings were about 207 billion tons in China, of which the total amount of tailings produced in 2018 was about 12.11 billion tons. Among all types of tailings, iron ore tailings have the largest amount of production, about 4.76 billion tons, accounting for about 39.31% of the total tailings production (Huang et al. 2020).

Therefore, it is imperative to explore new technologies for reducing iron ore tailings and their reuse as raw materials to produce value-added products. Recently, a promising application of iron ore tailings is its utilize as adsorbents or catalysts to remove dye compounds (Silva et al. 2011; Augusto et al. 2018), e.g. as a raw/regenerated efficient Fenton and Fenton-like catalysts for wastewater treatment. Given the high iron contents observed in iron ore tailing, it is reasonable to assume that these wastes are good catalysts for Fenton or Fenton-like processes (Augusto et al.

To whom correspondence should be addressed (caoyijun@163.com; lishuleibgs@163.com)

2018). However, Fe^{2+} is the effective state for activating the oxidant, while the most common state in iron waste is Fe^{3+} (dos Santos et al. 2016), and the presence of Fe^{3+} modifies the degradation rate(reaction time as long as 24 h) of substance. Some researchers got significant progress in trying to enhance the pollutant oxidation rate through reducing Fe^{3+} to Fe^{2+} (Augusto et al. 2018; de Freitas et al. 2019). Freitas *et al* achieved good results (80% dye decomposed with 3 h reaction) for the oxidation of methylene blue when iron ore tailing pretreated in a CH_4 atmosphere at 550 ℃ for 2 h.

Better degradation results could be achieved in case of iron waste pretreatment under reducing atmosphere (H_2, CO, CH_4). Biomass could produce reducing gases and compounds during pyrolysis (Williams and Besler 1996; Wang et al. 2010). In our previous paper, we found that a unite mass wheat straw could produce about 5 mg/g H_2 and 18 mg/g CH_4 (Gao and Goldfarb 2019). Therefore, if iron tailings and wheat straw blends were pretreated through pyrolysis to realize the conversion of ferric iron to a low-valent state, it would not only improve the catalytic oxidation efficiency of organic matter, but also realize the resource utilization of wheat straw, which is of great significance.

Therefore, this paper applies methylene blue as a model pollutant to investigate the influence of pyrolysis conditions on the catalyzed degradation rate of pollutants. The pyrolyzed products' morphology, physical-chemical properties, stability and the catalytic mechanism were discussed. The research in this article aims to provides a theoretical basic for iron ore tailing catalyst with high degradation rate.

2 Materials and methods

2.1 Materials

Iron ore tailings were kindly provided by “Hainan mining” industry, located in Hainan, China. The sample was hematite tailings (T), and ground to 74 μm prior to use. Wheat straw selected as biomass because of the high production in China, which was ground in a coffee mill and sieved to a particle size between 100 and 300 μm (Gao and Goldfarb 2019). Table S1 showed the characteristics of wheat straw and hematite tailings. Methylene blue was purchased from Aladdin Chemical Reagent Co.Ltd. China.

2.2 Synthesis of the catalysts

Hematite tailings and wheat straw mixed with mass ratio 1:1, 2:1, 3:1, 4:1 and 5:1. Then, these mixtures were treated in tube furnace using a heating rate of 10 °C /min(Wang *et al* found feedstock pyrolyzed at this heating rate could produce more reducing gas, such as CO and H_2) (Wang et al. 2018) until different temperatures (500, 600, 700, 800 and 900 °C) for different holding times (30, 45, 60, 90 and 120 min). The obtained catalyst was denoted as I/W(a:b)-T-t, where I iron ore tailings, W wheat straw, a:b the mass ratio (w/w), T finally temperature, t holding time.

2.3 MB decomposition experiments

To evaluate the decomposition rate of catalyst produced from iron ore tailings, the bath catalytic experiments were carried out using 0.3 g of pyrolyzed product in contact with 100 mL dye solution with initial concentration of 60 mg/L and 16 mmol H_2O_2 under a shaker. 1.5 mL of solution was pipetted at given time intervals, centrifuged for 1 min and the dye concentration was detected by a UV-vis spectrophotometer (Unico

UV-2800) at 664 nm.

To investigate the stability and reusability of catalyst, the optimal pyrolyzed product was reused/recycled several times for the MB decomposition under the same Fenton-like condition.

2.4 Analytical method

The phase transformation of ferrochemical group in pyrolyzed solid was analyzed by XRD (Bruker D8 Advance, Germany). The morphology and composition were characterized by SEM-EDX (FEI QuantaTM 250, USA). The textural properties were test by BET (BELSORP-max, Japen). The functional groups of catalysts were investigated by FTIR (Bruker Vertex 80v, Germany). Electron paramagnetic resonance (EPR, Bruker 300E spectrometer, Germany) was applied to test the main reactive oxidative species (ROS) generated in the system. Fe valence and carbon functional group variation of catalysts were characterized by XPS (Thermo Fisher Escalab 250 Xi, USA), and the C1s1/2(284.6 eV) was used as the binding energy calibration standard.

3 Results and discussion

3.1 Determination of optimal pyrolysis based on degradation rate

The pyrolysis preparation mass ratio (iron ore tailings to wheat straw), reaction time and heating rate were fixed at 3:1, 60 min and 10 ℃/min, respectively, and catalysts were obtained under different pyrolysis temperature. Fig.1(a) showed the comparison of MB removal efficiency versus time and pseudo-second-order kinetic constant (k_2, R^2>0.994) under different catalysts, which -5 min means the H_2O_2 was added after 5min adsorption. Only approximately 20% of MB was removed after 1 h

115 with a kinetic rate of 0.0139 min^{-1} when the product prepared at 500 °C used. However,
116 the removal rate and efficiency were substantially improved as the pyrolyzed
117 temperature increased. The best decomposition rate (0.0182 min^{-1}) and efficiency (74%)
118 were reached using a catalyst prepared at 900 °C, which was much higher than the
119 generated iron ore tailings catalyst reported by Augusto *et al* (7.4×10^{-4} min^{-1}, 63%)
120 (Augusto et al. 2018). Considering the dye decomposition rate and efficiency, the
121 optimal pyrolysis temperature for synthesizing catalyst was determined to be 900 °C.
122 Setting the pyrolysis temperature as 900 °C and final holding time as 60 min and
123 heating rate as 10 °C/min, the removal efficiency and rate of MB were investigated by
124 pyrolysis products at different mass ratio. As shown in Fig.1(b), only 10% MB was
125 removed with a removal rate k_2 of 0.0120 min^{-1} when the product prepared by hematite
126 tailings only, indicating that the pyrolyzed product synthesized from iron ore tailings
127 might not be active for dye degradation. While the decomposition efficiency of MB (k_2
128 increased from 0.0120 min^{-1} to 0.0182/0.0183 min^{-1}) gradually increased when the
129 products made from hematite tailings and wheat straw blends were used as catalyst.
130 This may be due to biomass blends helped to reduce the $\equiv Fe^{3+}$ to $\equiv Fe^{2+}$ or low-valent
131 iron (Ellison and Boldor 2021). The mechanism of H_2O_2 activation by iron ore tailings
132 based catalyst with $\equiv Fe^{2+}$ may involve the following reaction processes(Luo et al. 2010).
133 Firstly, a complex assigned as $\equiv Fe^{2+} \cdot H_2O_2$ may form between the hydrous surface of
134 $\equiv Fe^{2+} \cdot H_2O$ and H_2O_2(Eq.(1)), where $\equiv Fe^{2+} \cdot H_2O$ represents the reduced sites on the
135 iron ore tailings catalyst surface. The formed $\equiv Fe^{2+} \cdot H_2O_2$ can produce $\cdot OH$ by H_2O_2
136 activation, which is ready to decompose and oxidize MB(Eq.(2) and (3)).

$$\equiv \mathrm{Fe}^{2+} \cdot H_2O + H_2O_2 \rightarrow \equiv Fe^{2+} \cdot H_2O_2 \quad (1)$$

$$\equiv Fe^{2+} \cdot H_2O_2 \rightarrow \equiv Fe^{3+} + \cdot OH + OH^- \quad (2)$$

$$\cdot \mathrm{OH} + \mathrm{MB} \rightarrow \cdots CO_2 + \mathrm{H_2}O \quad (3)$$

However, the radical formation mechanism by $\equiv Fe^{3+}$ and H_2O_2 is proposed as follows:

$$\equiv Fe^{3+} + H_2O_2 \rightarrow Fe^{3+} \cdot H_2O_2 \quad (4)$$

$$\equiv Fe^{3+} \cdot H_2O_2 \rightarrow \equiv Fe^{2+} + \cdot OOH + H^+ \quad (5)$$

$$\equiv Fe^{3+} + \cdot \mathrm{OOH} \rightarrow \equiv Fe^{2+} + O_2 + H^+ \quad (6)$$

The formed $\equiv Fe^{2+}$ subsequently produce •OH (Eq.(1)-(3)). Although •OH can be generate from H_2O_2 when either $\equiv Fe^{2+}$ or $\equiv Fe^{3+}$ is present, the generation rates are much faster between $\equiv Fe^{2+}$ and oxidant (Kwan and Voelker 2002). Although the degradation efficiency for catalysts produced from mass ratio 1:1, 2:1 and 3:1 was equivalent, degradation rate k_2 values of mass ratio 3:1(0.0182 min^{-1}) and 2:1 (0.0183 min^{-1}) were higher than 1:1(0.0158 min^{-1}). In order to realize the iron ore tailings bulk utilization and construct a catalyst with higher degradation rate, we determined the optimal mass ratio of iron ore tailings to wheat straw was 3:1.

Fixing the pyrolysis temperature as 900 °C, the ratio of iron ore tailings to wheat straw as 3:1 and heating rate as 10 ℃/min, the optimum holding time was investigated in Fig.1(c). The dye decomposition efficiency of pyrolyzed product was enhanced when the holding time for the synthesis catalyst stretched from 30 to 60 min. However, the degradation efficiency of MB was not significantly improved when the holding time further extended to 90 and 120 min. Interestingly, k_2 showed a first increasing then

159 decreasing trend as the holding time extending, and reached the maximum (0.0182 min-
160 ^{1}) when the holding time was 60 min. Thus, 60 min was the optimal catalyst holding
161 time among those investigated parameters.

162 To sum up, the relative optimal pyrolysis condition was a blends ratio of 3:1, a
163 pyrolysis temperature of 900 °C and a holding time of 45 min. pH as an important factor
164 for the efficiency of Fenton-like reaction, the effect of pH was investigated in Fig 1(d).
165 We could see that pH could significantly affect the degradation of MB in iron ore
166 tailings catalyzed Fenton-like process. As shown in Fig.1(d), the degradation efficiency
167 was relatively low and the k_2 values were 0.0104 min^{-1} and 0.0182 min^{-1} at pH 8.1 and
168 6.8(did not adjust). While the decomposition of MB gradually increased as the pH value
169 decreasing and got a highest/fastest degradation efficiency (84% MB removal, 0.0229
170 min^{-1}) at around pH 3, which was consistent with previous studies (Hu et al. 2011). The
171 generation of •OH from H_2O_2 is the key step in the entire Fenton-like process,
172 and •OH catalyzed by iron ore tailings are gradually limited with pH increasing. The
173 higher pH with more OH^- will cause the reaction (Eq. (7)) to shift back and reduce the
174 activity of Fenton reagent (Zheng et al. 2016), which resulted in a slow decomposition
175 rate of I/W(3:1)-900-60.

176 $$Fe^{2+} + H_2O_2 \leftrightarrow Fe^{3+} + OH^- + \cdot OH \qquad \text{Eq.(7)}$$

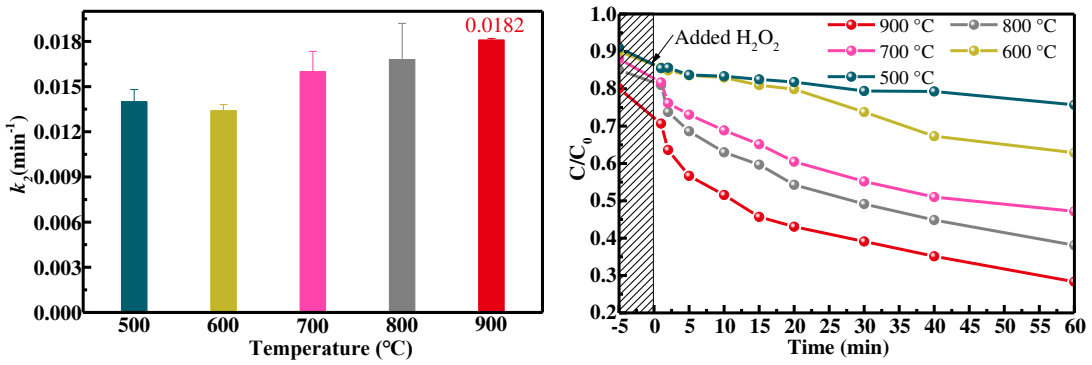

(a) Pyrolyzed temperature

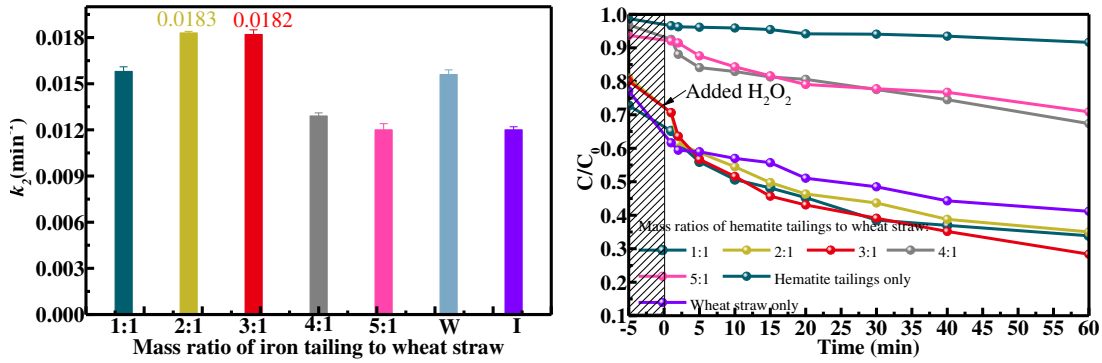

(b) Iron ore tailings to biomass mass ratio

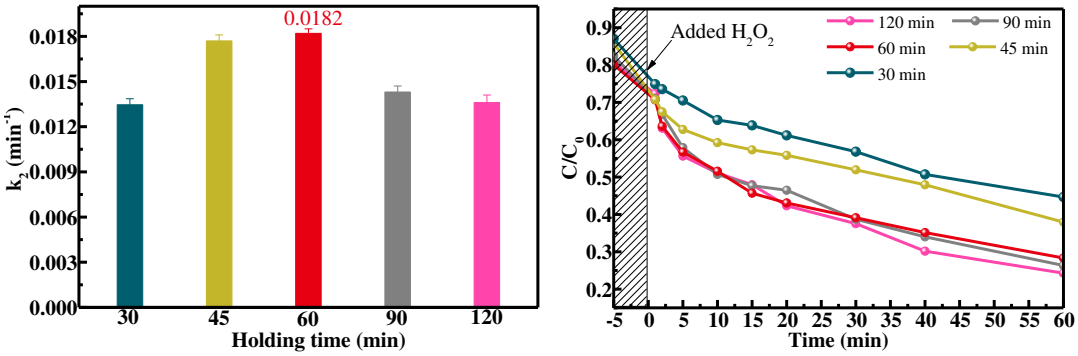

(c) Holding temperature

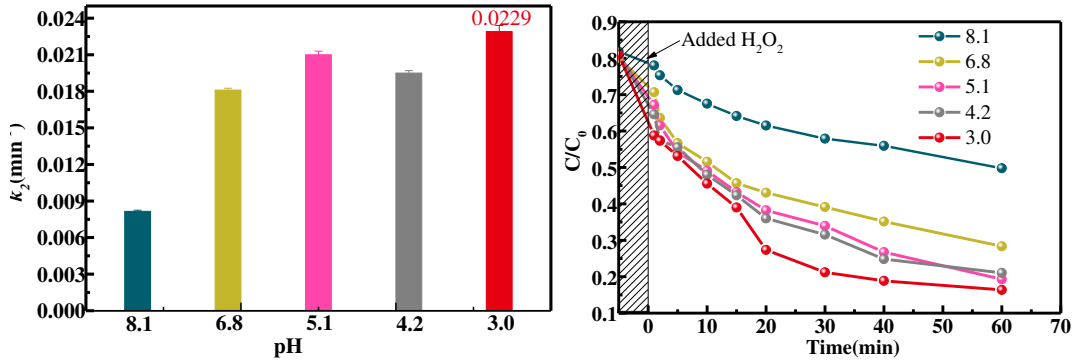

(d) pH value

Figure 1 Degradation of MB by pyrolyzed product prepared under different conditions

3.2 Catalyst characterization

Since the catalytic efficiency was apparently different by I-900-60, WS-900-60 and I/W(3:1)-900-60, XRD patterns were collected to indicate the phase information of these samples, shown in Fig.2. The XRD pattern of I/W(3:1)-900-60 showed diffraction peaks at 2θ=30.3°, 43.3°, 53.8°, 57.5°, 68.2° corresponded to Fe_3O_4, which exhibits magnetic characteristics. The peaks of WS-900-60 were noted at 2θ=21.8°, 26.5°, 28.0°, corresponding to SiO_2 crystallites. The diffraction peaks of raw iron ore tailings (RT) were attributed to α-FeOOH, and α-FeOOH was converted to Fe_2O_3 when heated to 900 °C under N_2 atmosphere (Zhang et al. 2018). Therefore, only the pyrolysis of iron ore tailings or wheat straw cannot produce a composite with low-valent iron.

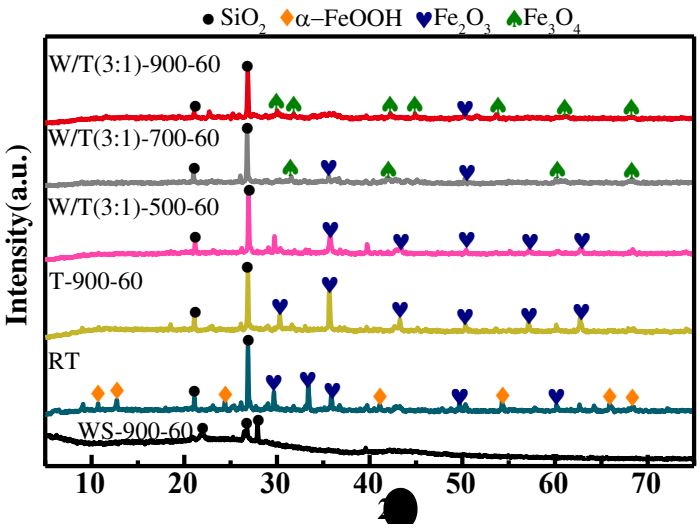

Figure 2 XRD patterns of the raw and prepared samples

Significant transformation of Fe_2O_3 to Fe_3O_4 was observed at 700-900 °C. When the temperature reached above 700 °C, most of Fe_2O_3 peaks disappeared, and the diffraction peaks of magnetite appeared. It can be concluded that Fe_2O_3 with trivalent could be reduced to Fe_3O_4 during high-temperature pyrolysis. More Fe_2O_3 spindles were converted to Fe_3O_4 as the temperature increasing. This might due to that there were organic matters such as cellulose, hemicellulose and lignin in wheat straw, and

these organic matters could be cracked and devolatilized into reducing gas or liquid, such as H_2, CH_4, which lead to the ferric iron reduction (Gong et al. 2012; Sharma et al. 2015; Xun et al. 2019; Yunji et al. 2019). In summary, in the process of co-pyrolysis of wheat straw and iron ore tailings, the reducing substances such as H_2 or CH_4 produced from wheat straw exhibited strong reducibility to reduce iron ore tailings to magnetite. Furthermore, the reduction degree increased as temperature increasing.

To illustrate the effect of biomass/wheat straw on the high degradation efficiency catalyst formation, the morphologies of I-900-60 and I/W(3:1)-900-60 were further compared. The surface morphologies of I-900-60 and I/W(3:1)-900-60 were shown in Fig.S1. The I-900-60 presented a large flaky structure with a flat and non-porous surface after pyrolysis, mainly because the natural structure of iron ore tailings. In the case of I/W(3:1)-900-60, SEM images showed that most particles had a smaller flake structure, with porous surface. This result indicated that mixing wheat straw promote the formation of a porous and smaller flake structure.

Table 1 BET and BJH results of prepared catalysts

Samples	Surface area(m^2/g)	Pore volume(cc/g)	Average pore size(nm)
I-900-60	1.1963	0.2749	12.935
I/W(3:1)-900-60	24.319	5.5875	3.707

As observed from SEM images, I/W(3:1)-900-60 had a smaller particle than I-900-60. N_2 adsorption-desorption isotherm was applied to calculate the surface area, pore volume and pore size distribution. As shown in Table 1 and Fig.S2, the average pore size of T-900-60 and I/W(3:1)-900-60 was 12.95 nm and 3.707 nm. However, the total pore volume was 0.2749 cc/g and 5.5875 cc/g, respectively. Thus, we can conclude that wheat straw addition increased the pore volume, and decreased average pore size.

Additionally, although I/W(3:1)-900-60 had a much larger specific surface area(24.319 cm^2/g) than I-900-60(1.1963 cm^2/g), its surface area was smaller than those reported iron-load activated carbon adsorbent (300-600 m^2/g) (Park et al. 2015; He et al. 2016; Saleh et al. 2017). This result further verified that prepared catalysts from iron ore tailings had weak adsorption ability. Therefore, we speculated the MB degradation by I/W(3:1)-900-60 was due to catalysis instead of adsorption. I/W(3:1)-900-60, with relatively larger surface area and richer pore volume, could provide greater active catalysis sites and increase catalysis performance (Neamţu et al. 2004; Duarte et al. 2012), agreed with the improved MB degradation efficiency catalyzed by I/W(3:1)-900-60.

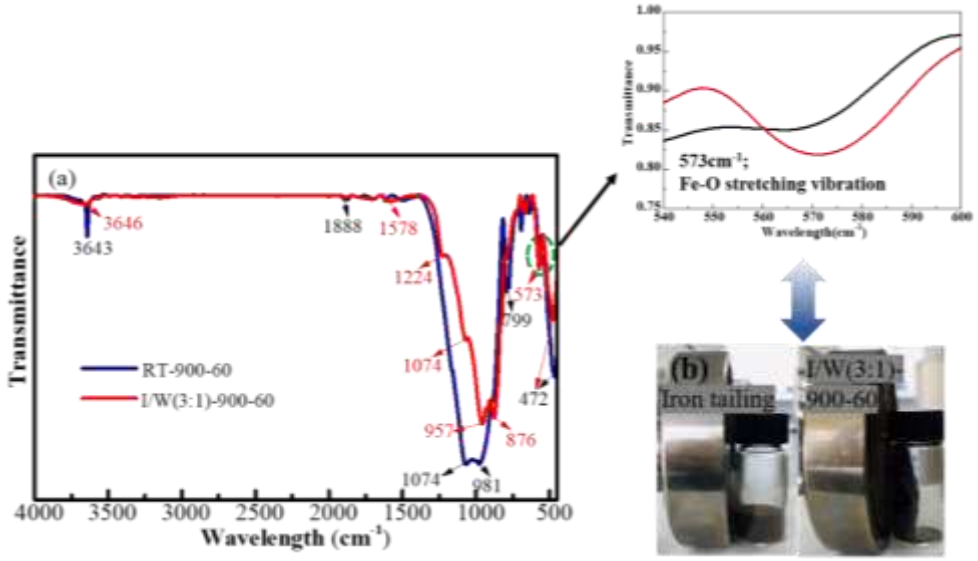

Figure 3 (a) the photos of the products attraction to a magnetic device; (b) FTIR spectra of I-900-60 and I/W(3:1)-900-60

There is an important question to further discuss that whether composites (wheat straw biochar and iron ore tailings) were simply mixed and exist alone or integrated together. Fig.3(a) showed the catalysts were attracted as a whole by a magnetic device, indicating iron ore tailings and biochar combined as a whole. This binding form is

beneficial to remove the catalyst from wastewater after reaction. In addition, FTIR spectra was shown in Fig.3(b). The peak at 3643/3646 cm^{-1} was attributed to O-H stretching and bending vibrations (Zhang et al. 2018). Similar I-900-60 peaks were observed in the spectra of both I-900-60 and I/W(3:1)-900-60, including Si-O stretching vibrations of the Si-O-Si, Si-O-Al, Si-O-Fe groups (1074 cm^{-1}, 957/981 cm^{-1}, 472 cm^{-1}), although their intensities varied (Doelsch et al. 2003). The silicon content in iron ore tailings was much higher than that in wheat straw (Table S1). Therefore, the intensity of Si-O stretching vibration in I-900-60 was stronger than in the spectrum of I/W(3:1)-900-60. Meanwhile, new peaks associated with the -C=O and -C-H stretching vibration at 1224 cm^{-1} and 876 cm^{-1} were observed in the spectrum of I/W(3:1)-900-60; these peaks were assigned mainly to the formation of small organic molecules (such as, phenol, furfural, styrene) that are devolatilized, oxidized or creaked from wheat straw during pyrolysis process. In addition, a new peak at 573 cm^{-1} attributed to an asymmetric Fe-O stretching vibration was observed. It might be caused by loading iron into biochar or Fe_3O_4 itself (Yuan and Dai 2014). Therefore, the new bond Fe-O on I/W(3:1)-900-60 may indicate the combination of iron and biochar occurred through chemical bonds.

3.3 The catalyst's stability and reusability analysis

It is important to evaluate the stability of a heterogeneous catalyst. As illustrated in Fig.S3, I/W(3:1)-900-60 was stable in first three runs and remained high MB degradation efficiency. At the 4^{th} run, the activity of I/W(3:1)-900-60 reduced slightly but the degradation efficiency still higher than 80%, showing the iron ore tailings based

catalyst can be reused for at least 4 Fenton-like cycles without significant activity loss. This slightly activity loss is probably due to the small molecules produced during MB degradation occupying part of the active sites, leading to a decrease in catalytic efficiency (Zhang et al. 2018). In addition, the concentration of leaching iron ions after first three runs was measured. As shown in Table S2, the concentration of leached iron was 0.089 mg/L, 0.085 mg/L, and 0.093 mg/L, which was only 0.8% of the iron content in I/W(3:1)-900-60. Low leached iron concentration also indicated heterogenous Fenton catalysis was the dominant reaction for MB removal (Gao et al. 2017). Meanwhile, XRD and SEM were applied to examine the structure stability of I/W(3:1)-900-60. As illustrated in Fig.S4, compared with fresh catalyst, the crystalline nature and morphology of used I/W(3:1)-900-60 did not change significantly. These results indicated that the cost-effective I/W(3:1)-900-60 was a promising heterogenous catalyst in Fenton-like catalytic degradation of organic wastewater due to its significant stability and reusability.

3.4 Reactive oxidative species and catalysis mechanism

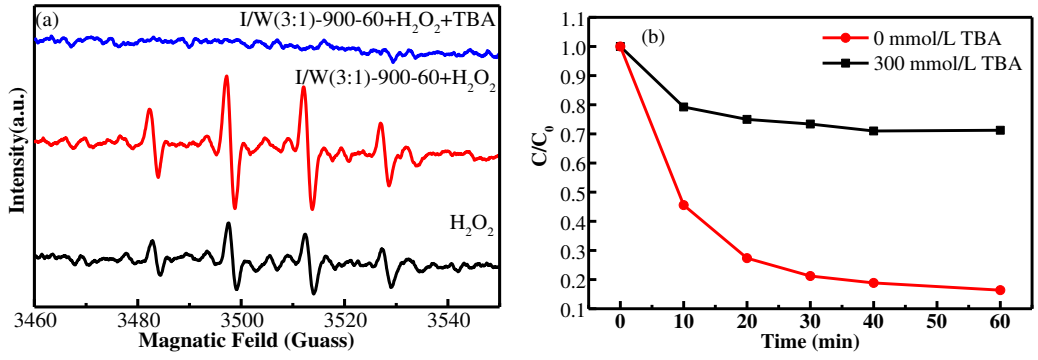

Figure 4 (a)DMPO-ROS adducts generated from I/W(3:1)-900-60 Fenton catalysis reactions at 10min (b)influence of radical scavenger (TBA) on the catalytic degradation of MB

ROS produced in I/W(3:1)-900-60 was detected by an EPR spin-trap technique

283 with DMPO. Fig.4(a) showed the EPR spectrum of the generated adducts during the 10
284 min reaction. On the EPR spectrum, there was observed a four-fold peak with an
285 intensity of 1:2:2:1, which was labeled to the DMPO-OH (Yang et al. 2013). However,
286 the four-fold peak was not appeared in the presence of 300 mmol/L T-Butyl alcohol
287 (TBA, • OH scavenger). Therefore, ·OH was the key ROS produced in I/W(3:1)-900-
288 60 catalyzed Fenton-like reactions. Fig.4(b) showed the effect of ·OH on MB
289 degradation. We can see the removal efficiency of MB significantly decreased from 84%
290 to 29% in the presence of 300 mmol/L. This result indicated that ·OH played a dominant
291 role in MB degradation in I/W(3:1)-900-60 catalyzed Fenton-like reactions.

292 The electron exchange between Fe(II)/Fe(III) and H_2O_2 can induce the formation
293 of • OH in the heterogeneous Fenton-like reaction. XPS was applied to analyze the
294 chemical state of iron species on I/W(3:1)-900-60 before and after catalysis reaction.
295 Fig. 5 shows XPS results of Fe2*p* in fresh and used I/W(3:1)-900-60. The peaks located
296 at 724.8 eV and 710.9 eV were attributed to Fe $2p_{1/2}$ and Fe $2p_{3/2}$ states of Fe*2p* orbits,
297 respectively (Gao et al. 2017; Li et al. 2018). Furthermore, the Gaussian-Lorentzian
298 was applied to decompose these two peaks into 6 different fitting peaks(Ding; et al.
299 2016). Among them, the fitting peaks located at 719.1 and 729.9 eV attribute to satellite
300 peaks, as well as at 712.0 and 725.3 eV assign to Fe^{3+}, and at 710.6 and 723.8 eV
301 correspond to Fe^{2+}, respectively (Li et al. 2018). A summary of deconvoluted peaks'
302 area and the Fe^{2+}/Fe^{3+} ratio was presented in Fig.5(a). Apparently, the ratio value of
303 Fe^{2+}/Fe^{3+} decreased from 2.18 to 2.17 after reaction, demonstrating only a small amount
304 of $\equiv Fe^{2+}$ lost electrons and oxidized to $\equiv Fe^{3+}$ during the catalysis reaction. These XPS

results are in accordance with the good recyclability and stability of I/W(3:1)-900-60 catalyst, which may attribute to the protective effects of the biochar (Li et al. 2018).

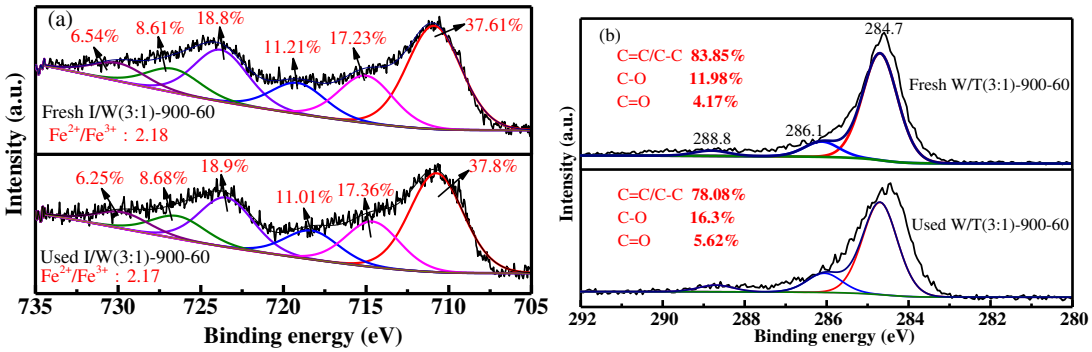

Figure 5 XPS spectra of Fe 2p(a) and C1s(b) on I/W(3:1)-900-60 before and after catalysis reaction

To further verify the protective role of biochar during Fenton-like reaction. XPS analysis was conducted to investigate the functional groups changes of I/W(3:1)-900-60 catalyst. As illustrated in Fig.5(b), the C1s spectra can be decomposed into three fitting peaks with C=C sp^2/C-Csp^3 (284.7 eV), C-O (286.1 eV) and C=O (288.8 eV) (Li et al. 2017b). Apparently, compared with the fresh I/W(3:1)-900-60, the relative content of C=C sp^2/C-Csp^3 carbon was reduced by 5.8%, C-O and C=O increased by 4.4% and 1.4% after catalysis reaction. This indicates that biochar was oxidized during the Fenton-like process with turning C=C sp^2/C-Csp^3 carbon to C-O or C=O. Therefore, the recyclability and stability of I/W(3:1)-900-60 catalyst may owe to the existence of biochar which acted as a sacrificial role and limited the oxidation of iron active sites in catalyst. Actually, the biochar can act as a catalyst with electron donor-accepter for the induction of H_2O_2 into $\cdot OH$ or $\cdot OOH$. The persistent free radicals (PFRs) on the surface of biochar formed by the thermal decomposition of organic compounds can be the reduced and oxidized active sites through electron transfer to form radical species ((Khachatryan and Dellinger 2011; Zhu et al. 2018). Fang *et al* found that PFRs on the

surface of biochar have an important influence on the production of OH by H_2O_2 activation (Fang et al. 2014). In addition, the PFRs on the biochar surface lead to the existence of unpaired electrons, which can exchange electrons directly with organic matter, accelerating the MB degradation efficiency (Fang et al. 2013; Yang et al. 2016).

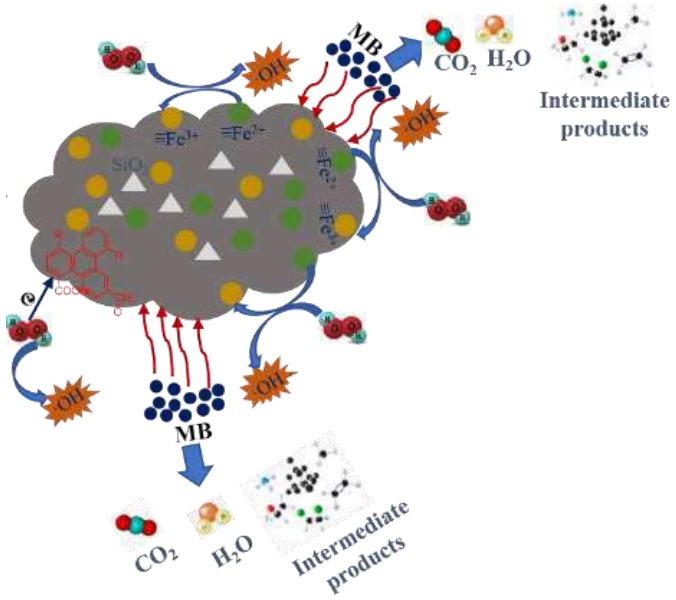

Figure 6 Proposed mechanism for Fenton catalysis reaction of I/W(3:1)-900-60

According to the above analysis results and discussion, the possible Fenton-like reaction mechanism was illustrated in Fig. 6. At the beginning, the MB molecules were adsorbed onto biochar of I/W(3:1)-900-60 from aqueous solution through surface action and pore diffusion. Then, the iron active sites of $\equiv Fe^{2+}$ and PFRs in biochar simultaneously transfer electron to H_2O_2 to generate ·OH for MB degradation. Moreover, the electron transfer between PFRs and iron active sites or the redox cycles of $\equiv Fe^{3+}/Fe^{2+}$ combined results in the enhanced degradation efficiency and rate of heterogenous Fenton-like reaction. Significantly, the stable performance of I/W(3:1)-900-60 with good reusability is due to the sacrificial effect of biochar for limiting the oxidation of iron active sites. In addition, the presence of unpaired electrons in PFRs

contributes to a certain extent to improve the degradation efficiency of pollutants. Table 2 showed the MB decompose rate k_2 for various Fenton-like catalysts. We can see that I/W(3:1)-900-60(0.0229 min^{-1}) exhibited *a* higher k_2 than or comparable to most reported kinetic rate data, which indicates that the co-pyrolysis of iron ore tailings and biomass waste is an effective way to improve the degradation rate/efficiency of iron ore tailings based heterogeneous catalysts. Meanwhile, it is of great significant to realize the resource utilization of iron ore tailings. However, these kinetic rate dates are far less than the degradation rate of homogeneous Fenton catalysis (Gou et al. 2021). Thus, the performance optimization of iron ore tailings-based heterogeneous catalysts based on porous and low-valent iron still needs further studied.

Table 2 Comparison of MB removal by Fenton-like methods with different catalysts

Catalyst	MB (mg/L)	Catalyst dosage (g/L)	Time (min)	k (min^{-1})	Reference
I/W(3:1)-900-60	60	3	60	2.29×10^{-2}	This study
Fe_3O_4	100	3	30	1×10^{-3}	(Costa et al. 2008)
Fe_3O_4 /H_2/300/1h	100	3	30	4×10^{-3}	(Costa et al. 2008)
Fe_3O_4 /H_2/400/1h	100	3	30	2×10^{-2}	(Costa et al. 2008)
Ferrocene	10	0.372	120	6.17×10^{-3}	(Wang et al. 2014)
Fe_3O_4/rGO	10	0.3	120	2.6×10^{-3}	(Liu et al. 2013)
Fe_3O_4/SiO_2/C	50	1	140	3.6×10^{-2}	(Liu et al. 2013)
Fe_3O_4/CeO_2	100	1	120	2×10^{-2}	(Li et al. 2017a)
Fe_3O_4/galic acid/GO	64	1	200	1.2×10^{-2}	(Hua et al. 2017)
N,C/CuO-Fe_2O_3	75	0.1	180	1.08×10^{-2}	(Ren et al. 2019)
FeNi/C-300	30	1	30	1.05×10^{-2}	(Li et al. 2020)

4 Conclusions

An iron ore tailings-based Fenton-like catalyst(I/W(3:1)-900-60) with relative fast catalysis rate was constructed by co-pyrolysis(900 ℃, 60min holding time) of iron ore

tailings and wheat straw with mass ratio of 3:1. Compared with single pyrolyzed iron ore tailing, the catalytic efficiency and rate of I/W(3:1)-900-60 (0.0229 min^{-1},84%) were considerably enhanced for the decomposition of MB due to the electron transfer between biochar and iron active sites or the redox cycles of $\equiv Fe^{3+}/Fe^{2+}$. As a result of the sacrificial effect of biochar, oxidizing C=Csp^2 bonds and limiting the deactivation of iron active sites($\equiv Fe^{2+}$), I/W(3:1)-900-60 showed a good reusability and stability. Moreover, the presence of unpaired electrons in persistent free radicals (PFRs) of biochar accelerated the electron exchange and further enhanced the MB decomposition rate. This work opens up a way to synthesize an iron ore tailings-based Fenton-like catalyst with higher degradation rate, as well as realize the utilization of solid wastes.

Acknowledgement

L.Gao acknowledges the support of the Fundamental Research Funds for the Central Universities (Grant no. 2020QN37).

Author contributions

Lihui Gao: Writing-original draft, methodology, Data curation; Lizhang Wang: Writing-Reviewing and Editing; Shulei Li: Investigation, Sample preparation; Yijun Cao: Supervision and Editing.

Availability of data and materials: All data generated or analyzed during this study are included in this published article.

Declarations

Ethics approval and consent to participate: Not applicable

Consent for publication: Not applicable

Conflict of interest: The authors declare no competing interests.

References:

Augusto TDM, Chagas P, Sangiorge DL, Mac Leod TCDO, Oliveira LCA, Castro CS De (2018) Iron ore tailings as catalysts for oxidation of the drug paracetamol and dyes by heterogeneous Fenton. J Environ Chem Eng 6:6545–6553 . https://doi.org/10.1016/j.jece.2018.09.052

Batista ÉR, Carneiro JJ, Araújo Pinto F, dos Santos JV, Carneiro MAC (2020) Environmental drivers of shifts on microbial traits in sites disturbed by a large-scale tailing dam collapse. Sci Total Environ 738:1–12 . https://doi.org/10.1016/j.scitotenv.2020.139453

Costa RCC, Moura FCC, Ardisson JD, Fabris JD, R.M.Lago (2008) Highly active heterogeneous Fenton-like systems based on Fe0/Fe3O4 composites prepared by controlled reduction of iron oxides. Appl Catal B Environ 83:131–139

De Freitas VAA, Breder SM, Silvas FPC, Radino Rouse P, de Oliveira LCA (2019) Use of iron ore tailing from tailing dam as catalyst in a fenton-like process for methylene blue oxidation in continuous flow mode. Chemosphere 219:328–334 . https://doi.org/10.1016/j.chemosphere.2018.12.052

Ding C, Zeng Y, Cao L, Zhao L, Zhang Y (2016) Hierarchically porous Fe_3O_4/C nanocomposite microspheres via a CO_2 bubble-templated hydrothermal approach as high-rate and high-capacity anode materials for lithium-ion batteries. J Mater Chem A 4:5898–5908

Doelsch E, Masion A, Rose J, Stone WEE, Bottero JY, Bertsch PM (2003) Chemistry and structure of colloids obtained by hydrolysis of Fe(III) in the presence of SiO_4 ligands.

Colloids Surfaces A Physicochem Eng Asp 217:121–128 . https://doi.org/10.1016/S0927-7757(02)00566-6

dos Santos PL, Guimarães IR, Mesquita AM, Guerreiro MC (2016) Copper-doped akaganeite: Application in catalytic Cupro-Fenton reactions for oxidation of methylene blue. J Mol Catal A Chem 424:194–202 . https://doi.org/10.1016/j.molcata.2016.08.034

Duarte F, Maldonado-Hódar FJ, Madeira LM (2012) Influence of the particle size of activated carbons on their performance as fe supports for developing fenton-like catalysts. Ind Eng Chem Res 51:9218–9226 . https://doi.org/10.1021/ie300167r

Ellison CR, Boldor D (2021) Mild upgrading of biomass pyrolysis vapors via ex-situ catalytic pyrolysis over an iron-montmorillonite catalyst. Fuel 291:120226 . https://doi.org/10.1016/j.fuel.2021.120226

Fang G, Gao J, Dionysiou DD, Liu C, Zhou D (2013) Activation of persulfate by quinones: Free radical reactions and implication for the degradation of PCBs. Environ Sci Technol 47:4605–4611 . https://doi.org/10.1021/es400262n

Fang G, Gao J, Liu C, Dionysiou DD, Wang Y, Zhou D (2014) Key role of persistent free radicals in hydrogen peroxide activation by biochar: Implications to organic contaminant degradation. Environ Sci Technol 48:1902–1910 . https://doi.org/10.1021/es4048126

Gao C, Chen S, Quan X, Yu H, Zhang Y (2017) Enhanced Fenton-like catalysis by iron-based metal organic frameworks for degradation of organic pollutants. J Catal 356:125–132 . https://doi.org/10.1016/j.jcat.2017.09.015

Gao L, Goldfarb JL (2019) Solid waste to biofuels and heterogeneous sorbents via pyrolysis of wheat straw in the presence of fly ash as an in situ catalyst. J Anal Appl Pyrolysis 137:96–

105 . https://doi.org/10.1016/j.jaap.2018.11.014

Gong X, Guo Z, Wang Z (2012) Effects of Fe_2O_3 on pyrolysis reactivity of demineralized higher rank coal and its char structure. Ciesc J 60:2321–2326 . https://doi.org/10.16552/j.cnki.issn1001-1625.2016.06.035

Gou Y, Chen P, Yang L, Li S, Peng L, Song S, Xu Y (2021) Degradation of fluoroquinolones in homogeneous and heterogeneous photo-Fenton processes: A review. Chemosphere 270:1–12 . https://doi.org/10.1016/j.chemosphere.2020.129481

He Q, Dai J, Zhu L, Xiao K, Yin Y (2016) Synthesis and lead absorption properties of sintered activated carbon supported zero-valent iron nanoparticle. J Alloys Compd 687:326–333 . https://doi.org/10.1016/j.jallcom.2016.06.139

Hu X, Liu B, Deng Y, Chen H, Luo S, Sun C, Yang P, Yang S (2011) Adsorption and heterogeneous Fenton degradation of 17α-methyltestosterone on nano Fe_3O_4/MWCNTs in aqueous solution. Appl Catal B Environ 107:274–283 . https://doi.org/10.1016/j.apcatb.2011.07.025

Hua Y, Wang S, Xiao J, Cui C, Wang C (2017) Preparation and characterization of Fe_3O_4/gallic acid/graphene oxide magnetic nanocomposites as highly efficient Fenton catalysts. RSC Adv 7:28979–28986

Huang D, Yan Q, Xue X, Ren Y, Shen Y (2020) Preparation of Iron Tailings-Based Porous Substrate and Its Application in Synthesis of Co_3O_4 Nanowires. Conserv Util Miner Resour 40:64–68

Khachatryan L, Dellinger B (2011) Environmentally persistent free radicals (EPFRs)-2. Are free hydroxyl radicals generated in aqueous solutions? Environ Sci Technol 45:9232–9239 .

https://doi.org/10.1021/es201702q

Kossoff D, Dubbin WE, Alfredsson M, Edwards SJ, Macklin MG, Hudson-Edwards KA (2014) Mine tailings dams: Characteristics, failure, environmental impacts, and remediation. Appl Geochemistry 51:229–245 . https://doi.org/10.1016/j.apgeochem.2014.09.010

Kwan WP, Voelker BM (2002) Decomposition of hydrogen peroxide and organic compounds in the presence of dissolved iron and ferrihydrite. Environ Sci Technol 36:1467–1476 . https://doi.org/10.1021/es011109p

Li D, Yang T, Li Y, Liu Z, Jiao W (2020) Facile and green synthesis of highly dispersed tar-based heterogeneous Fenton catalytic nanoparticles for the degradation of methylene blue. J Clean Prod 246:1–11

Li K, Zhao Y, Song Ch, Guo X (2017a) Magnetic ordered mesoporous Fe_3O_4/CeO_2 composites with synergy of adsorption and Fenton catalysis. Appl Surf Sci 425:526–534

Li S, Gao L, Wen H, Li G, Wang Y (2017b) Modification and application of coking coal by alkali pretreatment in wastewater adsorption. Sep Sci Technol 52:2532–2539 . https://doi.org/10.1080/01496395.2017.1355383

Li W, Wu X, Li S, Tang W, Chen Y (2018) Magnetic porous Fe_3O_4/carbon octahedra derived from iron-based metal-organic framework as heterogeneous Fenton-like catalyst. Appl Surf Sci 436:252–262 . https://doi.org/10.1016/j.apsusc.2017.11.151

Liu W, Qian J, Wang K, Xu H, Jiang D, Liu Q, Yang X, Li H (2013) Magnetically Separable Fe_3O_4 Nanoparticles-Decorated Reduced Graphene Oxide Nanocomposite for Catalytic Wet Hydrogen Peroxide Oxidation. J Inorg Organomet Polym Mater 23:907–916 . https://doi.org/10.1007/s10904-013-9863-4

Luo W, Zhu L, Wang N, Tang H, Cao M, She Y (2010) Efficient removal of organic pollutants with magnetic nanoscaled $BiFeO_3$ as a reusable heterogeneous fenton-like catalyst. Environ Sci Technol 44:1786–1791 . https://doi.org/10.1021/es903390g

Neamţu M, Zaharia C, Catrinescu C, Yediler A, Macoveanu M, Kettrup A (2004) Fe-exchanged Y zeolite as catalyst for wet peroxide oxidation of reactive azo dye Procion Marine H-EXL. Appl Catal B Environ 48:287–294 . https://doi.org/10.1016/j.apcatb.2003.11.005

Park HS, Koduru JR, Choo KH, Lee B (2015) Activated carbons impregnated with iron oxide nanoparticles for enhanced removal of bisphenol A and natural organic matter. J Hazard Mater 286:315–324 . https://doi.org/10.1016/j.jhazmat.2014.11.012

Ren B, Miao J, Xu Y, Zhai Z, Dong X, Wang S, Zhang L, Liu Z (2019) A grape-like N-doped carbon/CuO-Fe_2O_3 nanocomposite as a highly active heterogeneous Fenton-like catalyst in methylene blue degradation. J Clean Prod 240:1–10

Rico M, Benito G, Salgueiro AR, Díez-Herrero A, Pereira HG (2008) Reported tailings dam failures. A review of the European incidents in the worldwide context. J Hazard Mater 152:846–852 . https://doi.org/10.1016/j.jhazmat.2007.07.050

Saleh TA, Naeemullah, Tuzen M, Sarı A (2017) Polyethylenimine modified activated carbon as novel magnetic adsorbent for the removal of uranium from aqueous solution. Chem Eng Res Des 117:218–227 . https://doi.org/10.1016/j.cherd.2016.10.030

Sharma A, Pareek V, Zhang D (2015) Biomass pyrolysis - A review of modelling, process parameters and catalytic studies. Renew Sustain Energy Rev 50:1081–1096 . https://doi.org/10.1016/j.rser.2015.04.193

Silva AC, Cepera RM, Pereira MC, Lima DQ, Fabris JD, Oliveira LCA (2011) Heterogeneous

488 catalyst based on peroxo-niobium complexes immobilized over iron oxide for organic
489 oxidation in water. Appl Catal B Environ 107:237–244 .
490 https://doi.org/10.1016/j.apcatb.2011.07.017
491 Wang D, Xiao R, Zhang H, He G (2010) Comparison of catalytic pyrolysis of biomass with
492 MCM-41 and CaO catalysts by using TGA-FTIR analysis. J Anal Appl Pyrolysis 89:171–
493 177 . https://doi.org/10.1016/j.jaap.2010.07.008
494 Wang Q, Tian S, Ning P (2014) Degradation Mechanism of Methylene Blue in a Heterogeneous
495 Fenton-like Reaction Catalyzed by Ferrocenc. Ind Eng Chem Res 53:643–649
496 Wang X, Zhao H, Li Y, Song Q, Shu X (2018) Study on releasing characteristics of pyrolysis gas
497 products and kinetic analysis of lignite pyrolysis at different heating rates based on TG-MS.
498 Coal Eng 50:140–144
499 Williams P., Besler S (1996) The influence of Temperature and Heating rate on the Slow
500 Pyrolysis of Biomass. Renew Energy 7:233–250
501 Xun T, Jianan Z, Xuekai J, Bao W (2019) Catalysis of Fe2O3 for coal char pyrolysis. J WUhan
502 Univ Sci Technol 42:117–120
503 Yang J, Pan B, Li H, Liao S, Zhang D, Wu M, Xing B (2016) Degradation of p-Nitrophenol on
504 Biochars: Role of Persistent Free Radicals. Environ Sci Technol 50:694–700 .
505 https://doi.org/10.1021/acs.est.5b04042
506 Yang XJ, Xu XM, Xu J, Han YF (2013) Iron oxychloride (FeOCl): An efficient fenton-like
507 catalyst for producing hydroxyl radicals in degradation of organic contaminants. J Am Chem
508 Soc 135:16058–16061 . https://doi.org/10.1021/ja409130c
509 Yi L, Mi H, Wu Q, Xia J, Zhang B (2020) Present Situation of Comprehensive Utilization of

510 Tailings Resources in China. Conserv Util Miner Resour 3:814–815 .
511 https://doi.org/10.1038/163814b0
512 Yuan SJ, Dai XH (2014) Facile synthesis of sewage sludge-derived mesoporous material as an
513 efficient and stable heterogeneous catalyst for photo-Fenton reaction. Appl Catal B Environ
514 154–155:252–258 . https://doi.org/10.1016/j.apcatb.2014.02.031
515 Yunji P, Yue X, Yisheng C, Shengqiang S, Wuzhen Y, Xueli W (2019) Experimenal study on
516 catalytic pyrolysis pf pine sawdust added with Fe_2O_3. J Therm Sci Technol 18:185–190
517 Zhang H, Xue G, Chen H, Li X (2018) Magnetic biochar catalyst derived from biological sludge
518 and ferric sludge using hydrothermal carbonization: Preparation, characterization and its
519 circulation in Fenton process for dyeing wastewater treatment. Chemosphere 191:64–71 .
520 https://doi.org/10.1016/j.chemosphere.2017.10.026
521 Zheng J, Gao Z, He H, Yang S, Sun C (2016) Efficient degradation of Acid Orange 7 in aqueous
522 solution by iron ore tailing Fenton-like process. Chemosphere 150:40–48 .
523 https://doi.org/10.1016/j.chemosphere.2016.02.001
524 Zhu S, Huang X, Ma F, Wang L, Duan X, Wang S (2018) Catalytic Removal of Aqueous
525 Contaminants on N-Doped Graphitic Biochars: Inherent Roles of Adsorption and Nonradical
526 Mechanisms. Environ Sci Technol 52:8649–8658 . https://doi.org/10.1021/acs.est.8b01817
527

Supplementary Files

This is a list of supplementary files associated with this preprint. Click to download.

- SI.docx